Submitted to: ICIS '97
Seventh International Conference
on Ion Sources 9/7-13/97 BNL-64733

# A PLASMA WINDOW FOR VACUUM - ATMOSPHERE INTERFACE AND FOCUSING LENS OF SOURCES FOR NON-VACUUM ION MATERIAL MODIFICATION*

Ady Hershcovitch

AGS Department, Brookhaven National Laboratory

Upton, New York 11973-5000

Material modifications by ion implantation, dry etching, and micro-fabrication are widely used technologies, all of which are performed in vacuum, since ion beams at energies used in these applications are completely attenuated by foils or by long differentially pumped sections, which are currently used to interface between vacuum and atmosphere. A novel plasma window, which utilizes a short arc for vacuum-atmosphere interface has been developed. This window provides for sufficient vacuum atmosphere separation, as well as for ion beam propagation through it, thus facilitating non-vacuum ion material modification.

*Work performed under the auspices of the U.S. Department of Energy.

## I. INTRODUCTION

Material modification by ion implantation, dry etching, and micro-fabrication are performed exclusively in vacuum nowadays, since the ion guns and their extractors must be kept at a reasonably high vacuum. Two major shortcomings of material modification in a vacuum are low production rates due to required pumping time and limits the vacuum volume sets on the size of materials to be modified.

A novel apparatus,[1] which utilized a short plasma arc, was successfully used to maintain a pressure of 7.6 x exp(-6) Torr in a vacuum chamber with a 2.36mm aperture to atmosphere, i.e., a plasma was successfully used to "plug" a hole to atmosphere while maintaining a reasonably high vacuum in the chamber. Successful transmission of charged particle beams from a vacuum through the plasma to atmosphere was accomplished.[1] In addition to sustaining a vacuum atmosphere interface, the plasma has very strong lensing effect on charged particles. The plasma current generates an azimuthal magnetic field which exerts a radial Lorentz on charged particles moving parallel to the current channel. With proper orientation of the current direction, the Lorentz force is radially inward. This feature can be used to focus in beams to a very small spot size, and to overcome beam dispersion due to scattering by atmospheric atoms and molecules. Relatively hot plasma at the atmosphere boundary rarefies the atmospheric gases to further enhance ion beam propagation to the materials to be modified. Recent experimental results, with a plasma window coupled to a venturi, show a factor of three further enhancement in vacuum-atmosphere separation. Additionally, these recent results indicate that energy attenuation of ion beams in the plasma window (as they pass from vacuum to atmosphere) is substantially lower than what was estimated in the earlier work.[1]

Ion material modification by ion beams is performed exclusively in vacuum nowadays, since presently used vacuum-atmosphere interfaces for particle beam transmission, like foils or differential pumping, attenuate these ion beams completely. To rectify the shortcomings of present day vacuum-atmosphere interface, orifices and differentially pumped chambers (or foils) are to be replaced by a short high pressure arc, which interfaces between the vacuum chamber and atmosphere and has the additional advantage of focusing charged particle beams. Such an interface can facilitate non-vacuum ion material modification. The major advantages of this method and apparatus are higher production rates and elimination of size limitations.

## II. THEORY OF OPERATION

Plasmas can be used for vacua separation, interface with atmosphere, and as lenses. Three effects can enable a plasma to provide a rather effective separation between vacuum and atmosphere, as well as between vacua regions, and even act as a pump.

### IIa. Ideal Gas Pressure Effect

A most important effect is due to pressure equalization, whether it is between a discharge and atmosphere, or between a gas channel and atmosphere. Pressure is given by:

$$p = nkT \qquad (1)$$

Where n is the gas or the plasma density, k is the Boltzmann constant, and T is the temperature of the gas or the plasma. In some atmospheric arcs, e.g., like that used to test this effect experimentally, the axial plasma and gas temperature can be as high as 15000°K[2,3,4] with an average temperature as high as 12000°K. Based on Equation 1, to match atmospheric pressure at a room temperature of about 300°K, the arc plasma and gas density needs to be 1/40 of the room-temperature gas density. Therefore, a reduction in the vacuum chamber pressure by a factor of 40 is expected (since the chamber walls are close to room temperature).

## IIb. Dynamic Viscosity Effect

Viscosity increases with temperature. Consequently, reduction in gas flow through a hot plasma filled channel as compared to a room temperature gas filled channel is expected. Air flow, at atmospheric pressure, through a straight smooth tube of circular cross section with a very small diameter is laminar, hence, the Poiseuille equation[5] for the gas flow rate Q applies.

$$Q = \frac{\pi d^2}{16\eta \ell} p_a (p_1 - p_2) \quad , \tag{2}$$

where d and $\ell$ are the tube radius and length, $\eta$ is the gas viscosity, and $p_a$ is the arithmetic mean of $p_1$ and $p_2$. Since the viscosity of air increases with temperature,[6] it is clear from Equation 2 that air throughput decreases.

Some of the assumptions used to derive Equation 2 are no longer valid once a discharge is initiated, since the flow becomes compressible and nonisothermal.[4] Therefore, a thorough analysis of gas and plasma flow requires solution of coupled transport equations for ions and electrons, as well as the Naviar-Stokes equation for the gas. For electrons and ions, the relevant transport equations are the continuity and momentum transfer equations[7]

$$\frac{D}{Dt} n_{e,i} + n_{e,i} \nabla \cdot \underline{V}_{e,i} = 0 \quad , \tag{3}$$

$$\iota_{e,i} n_{e,i} \frac{D}{Dt} \underline{V}_{e,i} = -\nabla p_{e,i} - \nabla \cdot \underline{P}_{e,i} + q_{e,i} n_{e,i} [\underline{E} + \underline{V}_{e,i} x \underline{B}] + \underline{R}_{e,} \tag{4}$$

where m is the particle mass and q its charge. $\underline{R}$ is the species total momentum transfer, p its partial pressure and $\underline{P}$ is the stress tensor; and $D/Dt = \partial/\partial t + \underline{V} \cdot \nabla$ . The Naviar-Stokes equation is basically the momentum equation (Eq. 4) without the electric and magnetic field terms. It is usually written in a notation in which nm = $\rho$, $\underline{R} = \underline{f}$, and with a partially expanded stress tensor. To close this set of equations, more equations (e.g., energy transport) must be added and some assumptions must be made in order to truncate the equations. Solving this set of equations is beyond the scope of this paper. Nevertheless, it can be shown qualitatively, from this set of equations, that thermal effects play a significant role in reducing gas throughput through a plasma filled channel. The stress tensor $\underline{P}$ is directly proportional to the viscosity $\eta$, which in turn has a very strong temperature dependence.[6,7,8] For ions and electrons[7]

$$\eta_i = 2 \times 10^5 \mu^{1/2} \frac{k}{\lambda_i} T_i^{5/2} \quad , \quad and \ \ \eta_e = 2.5 \times 10^7 \frac{k}{\lambda_e} T_e^{5/2} \ . \qquad (5)$$

where $\lambda$ is the Coulomb logarithm and $\mu$ is the ion mass expressed in proton mass units. For gases, the simplest expression for viscosity is[6,8]

$$\eta = aT^x , \qquad (6)$$

where a and x are constant characteristics of each gas. For air, e.g., at about 1000°F, x is somewhat larger than 1. Consequently, the gas flow through a plasma filled channel should be greatly reduced, due to the strong enhancement in viscosity at high temperatures.

### IIc. Ionization Effect

A smaller contribution is expected from ionization of molecules and atoms by plasma particles and their subsequent confinement by the fields confining the plasma. A quick comparison between the ionization time [given by $(n_e\sigma v)^{-1}$, where $\sigma$ is the effective ionization cross section] for an atom or a molecule entering a 6 cm long, 2 mm diameter channel through which a 50 A 200 V electron current flows, and the atom or molecule transit time reveals that the ionization time is of the order of 0.1 μsec, while the transit time is of the order of 10s of μsec. Thus, the ionization probability is extremely high (but, recombination and wall effects reduce the ionization fraction to 15%-20%). This effect is very important in cases where gas flows are low. At steady state high flow rates, the plasma pressure will build up quickly and match the pressure exerted by the confining fields. This plasma accumulation creates the effective interface that was analyzed in the previous paragraphs. Additionally, this effect has a useful contribution to some applications by preventing metal chips and vapor from backstreaming into an electron beam column.

## IId. Plasma Lens

In a beam of charged particles, propagating through a field-free region, there are two forces acting on the particles: space charge forces trying to "blow" the beam up, and a magnetic force pinching the beam[9] (due to the magnetic field generated by the beam current). This magnetic force is a consequence of the Lorentz force, F, given by:

$$F = q\underline{V}x\underline{B} \tag{7}$$

Where q is the particle charge, V its velocity, and B is the magnetic field. When a beam enters a plasma, space charge forces are neutralized, hence, beam focusing results from the magnetic field. If the plasma carries a current, the resulting magnetic field must be added to Equation 7. In all cases of interest to this subject matter, currents generated in the arcs far exceed the beam currents.

## IIe. Ion Beam Focusing

Next, mathematical formalism is set up to facilitate focusing calculations for an ion beam as it propagates through a current carrying vacuum atmosphere interface. A fractional ionization of 15% is considered.[10] Scattering of beam ions by various particles and aberrations due to various beam formation elements lead to beam expansion. Both effects contribute to the beam transverse energy, $T_\perp$. Aberrations are a strong function of the particular geometry of source and beam formation element, whose contribution to the beam angular dispersion is given by G. The largest contribution to angular dispersion $\theta_g$ from gas scattering is dominated by multiple elastic scattering. This angular growth can be found in a number of text books.[11] Plasma ions, depending on the various parameters might be the dominant contribution to beam expansion. This angular growth $\theta_p$ can be estimated from derived relaxation rates. [12] The total angular rms growth $\Theta_t^2$ is, thus, given by

$$\Theta_t^2 = \theta_p^2 + \theta_g^2 + G$$

or in cgs units,

$$\Theta_t^2 = 48\pi e^4 n_p Z^2 (Z_i')^2 \lambda z/(pv)^2 + 4\pi e^4 n_g Z^2 Z'(Z'+1) z/(pv)^2 + G \qquad (8)$$

where n is density number, Z is the beam ion charge state, $Z_i'$ is the plasma ion charge state , Z' is the

atomic number of the gas species, $\lambda$ is the Coulomb Logarithm, p momentum, v velocity, and z is the distance traveled. The elementary charge is e.

Equation 8 can be used together with the beam envelope equation to calculate the growth in beam radius as a function of z. However, the objective of this work is to eliminate this growth by radially inward Lorentz acceleration. Mathematically, Equations 7 and 8 are employed to calculate effective electron transverse accelerations. Equating the two and solving for the magnetic field yields the plasma current required to accomplish this condition.

Inward acceleration, $\underline{a}_{\perp_i}$, by the Lorentz force can be calculated by dividing Equation 7 by the ion mass m.

$$\underline{a}_{\perp_i} = \frac{F}{m} = \frac{q}{m} \underline{V}_z x \underline{B}_\theta \tag{9}$$

Where $B_\theta$ is the azimuthal magnetic field generated by the plasma current I (the ion beam current is negligible for all cases of interest). Ampere's Law can be used to calculate $B_\theta$ at the outer radius, R, to yield

$$B_\theta = \frac{\mu_o I}{2\pi R}. \tag{10}$$

Substituting for $B_\theta$ in Equation 9 from Equation 10 yields

$$\underline{a}_{\perp_i} = \frac{q\mu_o}{2\pi R m} V_z I. \tag{11}$$

Outward transverse velocity growth can be calculated from Equation 8 to yield an effective outward acceleration $\underline{a}_{\perp_o}$,

$$\underline{a}_{\perp_o} = \mathrm{Fn}\left(\Theta_t^2\right) \tag{12}$$

i.e., the outward acceleration is a function of $\Theta_t^2$. Before solving equation 12, G form equation 8 must be determined. However, G depends on the particular geometry of an ion source and its beam forming elements. Arc current needed to prevent beam dispersion due to scattering can be obtained by equating Equations 11 and 12.

## IIf. Ion Beam Propagation

Collisions do not only scatter the beam, but also extract energy. [10] This effect dominates ion propagation, i.e., passage of ions through gas and plasma is dominated by slowing down interactions rather than transverse diffusion.

For many applications, e.g., microfabrication, ion beams with very small spot sizes (as low as 50 nm[13]) are used. Therefore, the ion beam passes through the channel axis, i.e., through the hottest part of the plasma and gas where the temperature is 15000°K. Thus, based on Equation 1, the helium gas density (from our newest results) at the interface with atmosphere is $n = 3.3 \times 10^{17} cm^{-3}$. And, for a 15% fractional ionization, the plasma density is $5 \times 10^{16} cm^{-3}$.

Examining plasma effects,[12] the fastest relaxation rate is slowing down of ions by plasma electrons (dynamic friction) given by[12]

$$\nu_s = 1.7 \times 10^{-4}\, n \lambda Z^2 \mu^{1/2} E^{-3/2} \quad . \qquad (13)$$

And, the forward velocity slowing down rate is $d\underline{V}_z / dt = -\nu_s \underline{V}_z$ .

For a 400 keV $Ga^+$ beam, Equation 13 yields $\nu_s = 4.3 \times 10^6 sec^{-1}$, and, since the ion velocity is $1 \times 10^8$ cm/sec at this energy, the energy attenuation rate is about 17 keV/cm; hence at the channel exit, the beam energy is expected to be of the order of 300 keV.

Ion attenuation by gas is also dominated by energy loss. The total energy loss can be calculated from the Bethe-Block equation[14,15]

$$\frac{dE}{dz} = \frac{4\pi e^4 Z^2}{m V^2} n Z' [\ell n \frac{2 m V^2}{W} - (1 - \beta^2) - \beta^2] \quad , \qquad (14)$$

where Z′ is the atomic number of the gas atoms and W is an empirical constant known as the geometric-mean ionization and excitation potential (of the order of 100 eV). For a 400 keV $Ga^+$ beam, Equation 14 yields an energy loss rate that is about 4 keV/cm.

## III. EXPERIMENTAL RESULTS

Two types of experiments were performed with a cascade arc discharge. The two types were a series of differential pumping experiments, and an electron beam propagation experiment. The later is not very relevant to this subject matter. Experimental details of the differential pumping experiments are presented in the following two sub-sections.

### IIIa. Differential Pumping Experiments With Conventional Gas Feed

Figure 1 shows the experimental setup that was used to determine the effectiveness of using an arc as a vacuum atmosphere interface. The arc is a wall-stabilized type cascade arc discharge[2,3,4] that was purchased from D. Schram's group at Eindhoven University of Technology. In this setup, the cathodes were at the atmospheric end of a channel that was 2.36 mm in diameter (0.093") and 6 cm long. A valve was mounted on an insulator. This valve was opened to atmosphere after discharge initiation and a subsequent elevation of $P_1$ to atmospheric pressure. The opposite end of the channel was opened to a pipe, pumped by a mechanical pump, on which the cascade arc was mounted. This pipe was connected to a box (partially shown in Figure 1) through a valve. The maximum arc current was 50 A (power supply limit). Pressure at $P_1$ and $P_2$ was measured with Granville-Phillips thermocouple gauges, and in addition, $P_1$ was also measured with a HEISH absolute mechanical pressure gauge that utilizes a Bourdon tube. A Perkin-Elmer ULTEX ionization gauge was used to measure $P_3$.

Using only differential pumping and opening the valve to atmosphere with no discharge $P_1 = 760$ Torr and $P_2 = 80$ Torr was measured. After the discharge was initiated in argon, $P_1$ was set slightly above atmosphere, and the valve was opened. As the arc current was raised from 10 A to 50 A, the pressure at $P_2$ decreased with increasing arc current, reaching 350 mTorr at 50 A. This represents a **reduction by a factor of 228.6 over differential pumping.**

Figure 2 shows the pressures $P_2$ and $P_3$ as a function of the arc current for discharge in argon, $P_1$ was at 760 Torr. Next, the gas feed was switched to helium, and the same measurements were repeated with helium as the discharge gas. The results were similar, although the pressures at $P_2$ and $P_3$ were higher by a factor of about 2.8 for the same arc currents.

Qualitatively, the results displayed in Figure 2 are consistent with the theoretical arguments introduced in the previous section. The plasma and gas temperatures are known to increase with increasing arc current.[2,3,4] Therefore, the plasma and gas viscosities are expected to rise with increase in arc current, while the channel gas density is expected to decrease with increasing arc current. Consequently, $P_2$ and $P_3$, as expected, decrease with increasing arc current. Quantitatively, based on some previous temperature measurements, [2,3,4] the plasma and gas temperature can be of the order of 12000°K. Hence, for a room temperature of about 300°K, the effect based on Equation 1 accounts for a factor of 40 in pressure reduction at $P_2$. The extra factor of 5.7 reduction in $P_2$ is most likely due to increase in viscosity and momentum transfer.

### IIIb. Differential Pumping Experiments With Venturi Gas Feed

Figures 3a and 3b are photos of an active experiment plasma window set up. On one side of a 4" diameter “T” is a plasma window (figure 3a), while on the opposite side there is a viewing port. Figures 4a and 4b are photos of the plasma in the window take from the atmosphere (4a) and through the viewing port (4b). A venturi (from the left, it is the first component with a gas feed) is novel feature, which is incorporated in this plasma window. More details of the venturi can be seen in figure 5. A convectron gauge is used to measure the pressure in the vacuum “T”.

Gas supply for this window is fed through the venturi. The rational for using the venturi is to utilize the gas to enhance the differential pumping. Experimentally, there was a further enhancement in the plasma window performance by another factor of 3, i.e., the difference in the pressure in the "T" (plasma window on versus plasma window off) was a factor of 600. Thus the **enhancement over differential pumping was a factor of 600** with the venturi (compared to 228.6 without the venturi). Additionally, with the venturi, there was a 25% reduction in power consumed by the plasma window arc. Obviously much of the enhancement can be attributed to pressure reduction at the cathodes. It is not clear whether there are other contributing factors (like higher temperature or enhanced viscosity).

## IV. DISCUSSION

A 2.3 mm diameter 6 cm long channel filled with helium or argon cascade arc discharge plasma was successfully used to establish a vacuum-atmosphere interface.

Computations carried out in this paper indicated that ions of interest to ion material modifications could be successfully transported through such a window, and retain sufficient energy to perform their task. Due to the large variety of ions and the wide range of ion energies used in material modifications, detailed analysis of ion beam attenuation and focusing is needed for each application. Nevertheless, since the principle of this type of focusing had been demonstrated,[16,17] and since data[18] indicates a reasonable range of ions in air, non-vacuum ion material modification seems feasible, with such a vacuum-atmosphere interface.

Among some of the benefits of using this type of vacuum-atmosphere windows are the increase in production rate, and the potential of performing various types of ion material modifications on large work pieces and in previously inaccessible places. An ion gun coupled to a plasma window is shown in Figure 5, the cooling plates can be miniaturized to provide for a long narrow discharge channel, to reach previously inaccessible places.

## V. ACKNOWLEDGMENTS

Many thanks to Daan Schram and his group at Eindhoven (especially Ries van de Sande) for help with the cascade arc device. Excellent technical support was provided by Whitey Tramm and Walt Hensel. Special thanks to Dave Langiulli for his support of this project. Contribution from students Peter Kollman and Alex Jeffers was invaluable in setting up the experiments and in data collection. Special thanks to my new collaborators Erik Johnson and Peter Stefan for their contributions to the new plasma window setup and experiments.

## VI. REFERENCES

[1] A. Hershcovitch, J. Appl. Phys. 78, 5283 (1995).

[2] C.J. Timmermans, R.J. Rosado, and D.C. Schram, Z. Naturforschung 40A, 81 (1985).

[3] G.M.W. Kroesen, D.C. Schram, and J.C.M. de Haas, Plasma Chemistry and Plasma Processing 10, 531 (1990).

[4] J.J. Beulens, D. Milojevic, D.C. Schram, and P.M. Vallinga, Phys. Fluids B, 3, 2548 (1991).

[5] L.D. Landau and E.M. Lifshitz, "Fluid Mechanics", Addison-Wesley Publishing Co., Reading, Mass., 1959.

[6] R.L. Daugherty and A.C. Ingersoll, "Fluid Mechanics", McGraw-Hill Book Co., Inc., 1954.

[7] S.I. Braginskii, "Transport Processes in a Plasma", Reviews of Plasma Physics, Vol. 1, (Consultants, Bureau, New York, 1965).

[8] S. Chapman and T.G. Cowling, "The Mathematical Theory of Non-Uniform Gases", Cambridge, England, The University Press, 1939.

[9] W.H. Bennett, Physical Review 45, 890 (1934).

[10] D.C. Schram, private communication, 1993; although this fractional ionization can be as high as 20%.

[11] Expressions derived from H.A. Bethe's work, e.g., J.D. Jackson, "Classical Electrodynamics", Second Edition, Wiley, New York, 1975. And B. Rossi, "High Energy Particles" Englewood Cliffs: Prentice-Hall, 1952.

[12] B.A. Trubnikov, "Particle Interactions in a Fully Ionized Plasma", Reviews of Plasma Physics, Vol. 1, (Consultants Bureau, New York, 1965).

[13] P.D. Prewett, Rev. Sci. Instrum. 63, 2364 (1992).

[14] H.A. Bethe, Ann. Physik 5, 325 (1930).

[15] H.A. Bethe, Z. Physik 76, 293 (1932).

[16] M. Giesch, B. Kuiper, B. Langeseth, S. Van Der Meer, D. Neet, G. Plass, G. Pluym, and B. De Raad, NIM 20, 58 (1963).

[17] C.L. Olson, J. Fusion Energy 1, 309 (1982).

[18] R.D. Evans, "The Atomic Nucleus", McGraw-Hill Co., New York, 1970; see, e.g., data in Chapt. 22 on range of α particles and fission fragments in air; J. Boggild, K. Bronstrom, and T. Lauritsen, Phys. Rev. 59, 275 (1941).

## FIGURE CAPTIONS

1. Schematic (not to scale) of the setup for the vacuum-atmosphere interface experiment. The cascade arc is enlarged to show details of its main components: cathodes and cooling plates. $P_2$ is measured in a 4" pipe, while $P_3$ is measured in a box whose dimensions are 2′ x 2.5′ x 4′.
2. With $P_1$ = 760 Torr, $P_2$ and $P_3$ are displayed as a function of the arc current in argon discharges.
3. Photos of the new experimental setup showing: (a) the plasma window, (b) view port.
4. Plasma channel photo taken: (a) from atmosphere, (b) through viewing port.
5. Schematic of an ion gun couple to a plasma window, which can be used for implantation etching, or micro-fabrication.

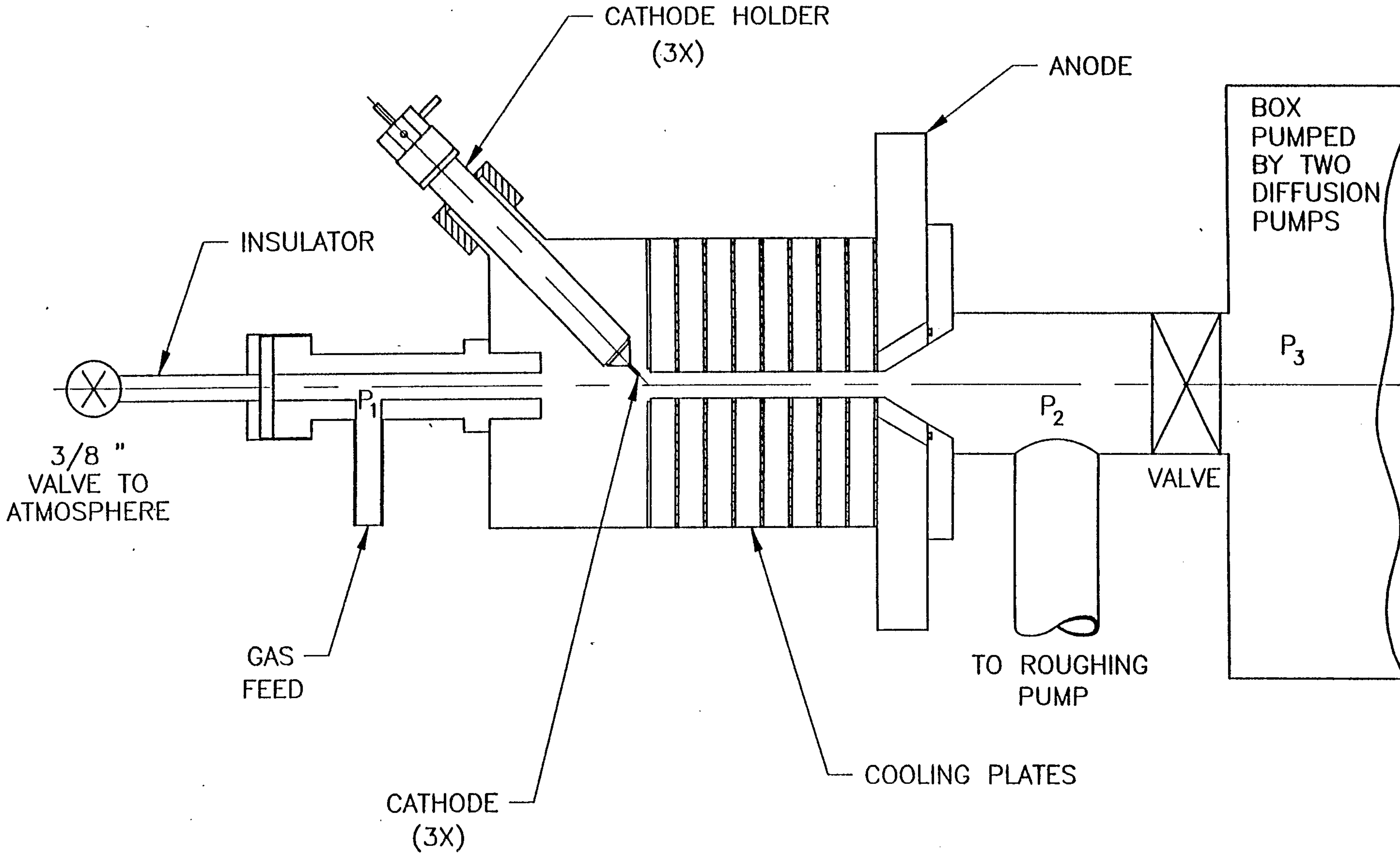
CATHODE HOLDER
(3X)
ANODE
BOX
PUMPED
BY TWO
DIFFUSION
PUMPS
INSULATOR
$P_3$
3/8 "
VALVE TO
ATMOSPHERE
$P_1$
$P_2$
VALVE
GAS
FEED
TO ROUGHING
PUMP
COOLING PLATES
CATHODE
(3X)

Figure 1

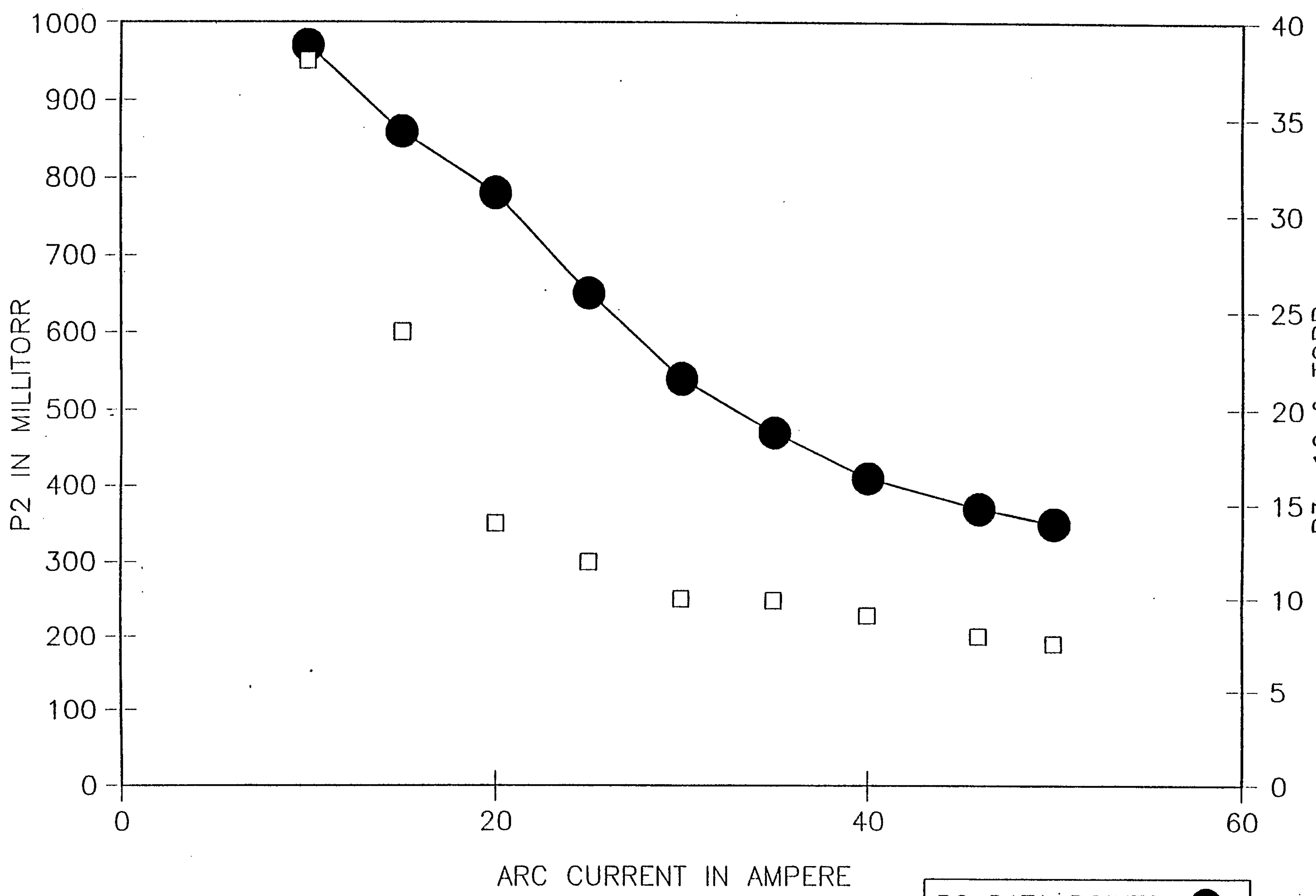


PRESSURE VERSUS CURRENT
FOR ARGON DISCHARGES

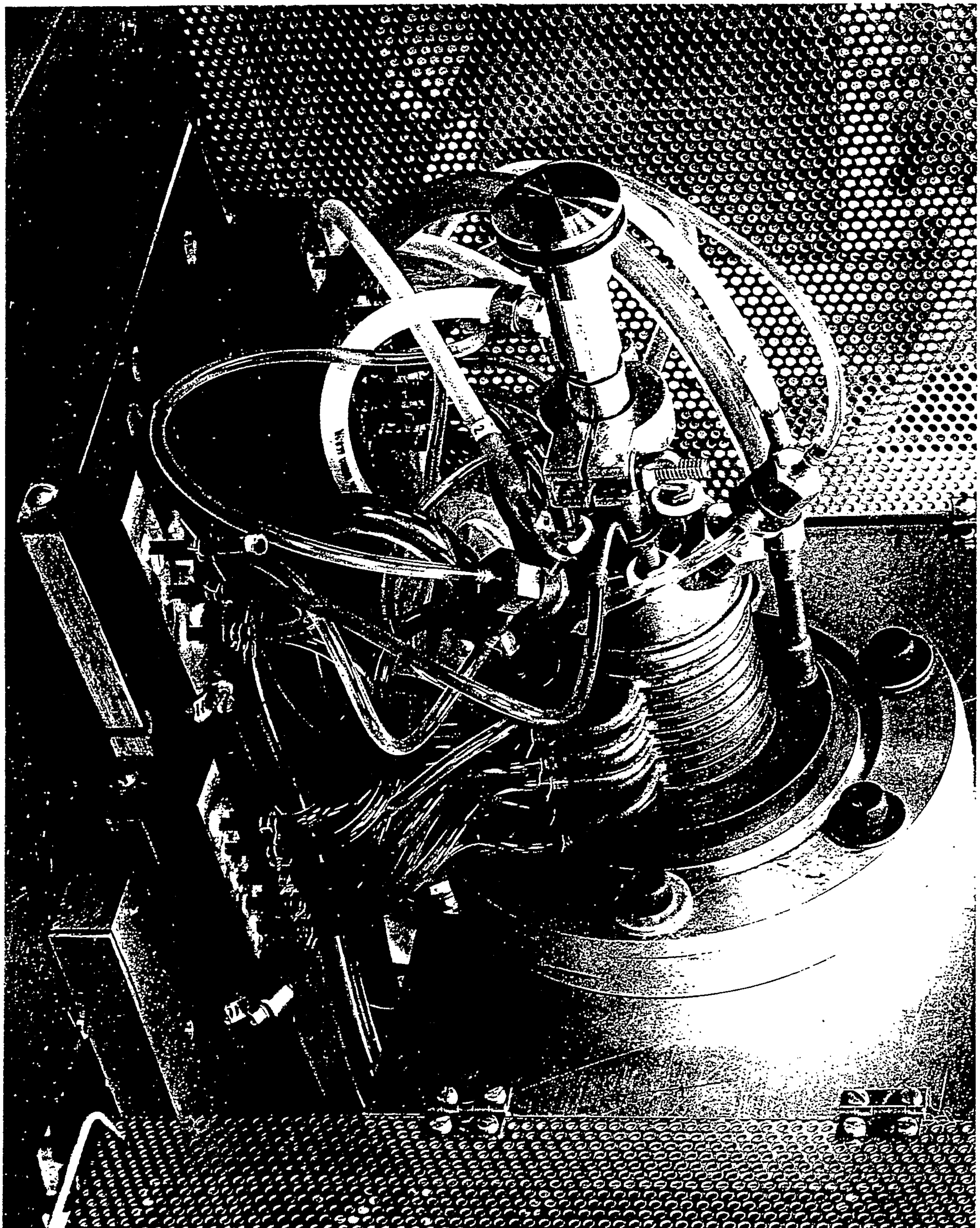

Figure 3a

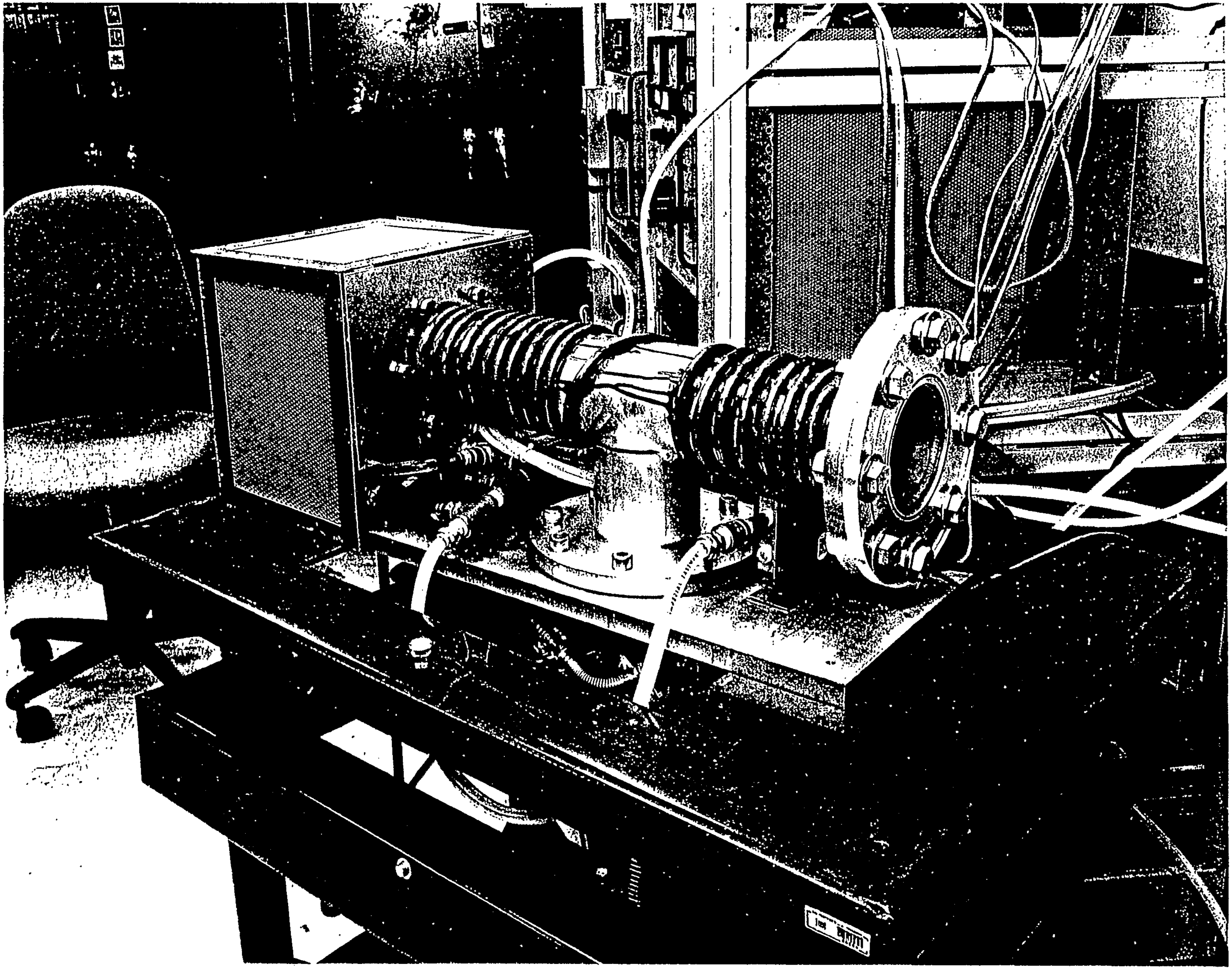

Figure 3b

Figure 4a

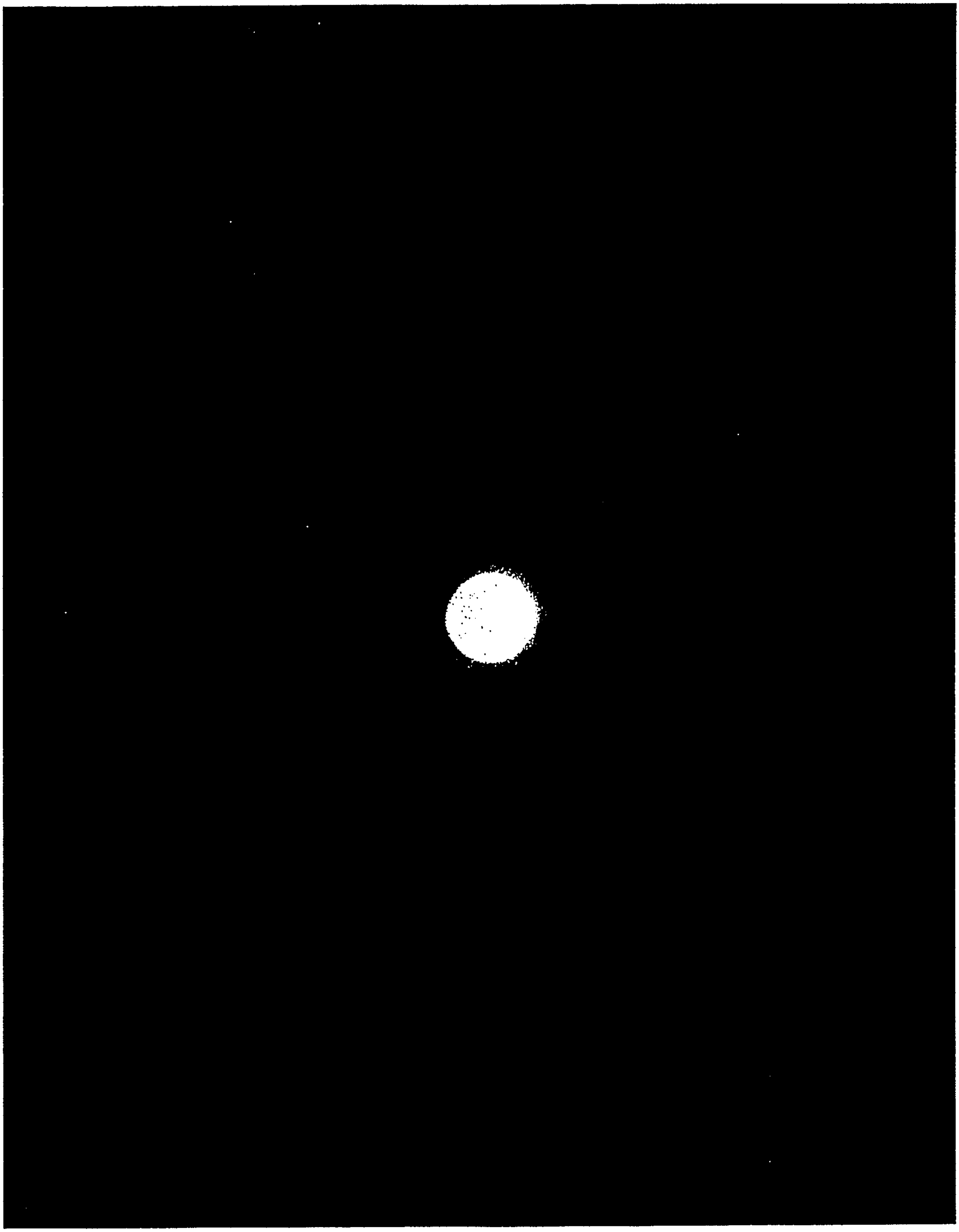

Figure 4b

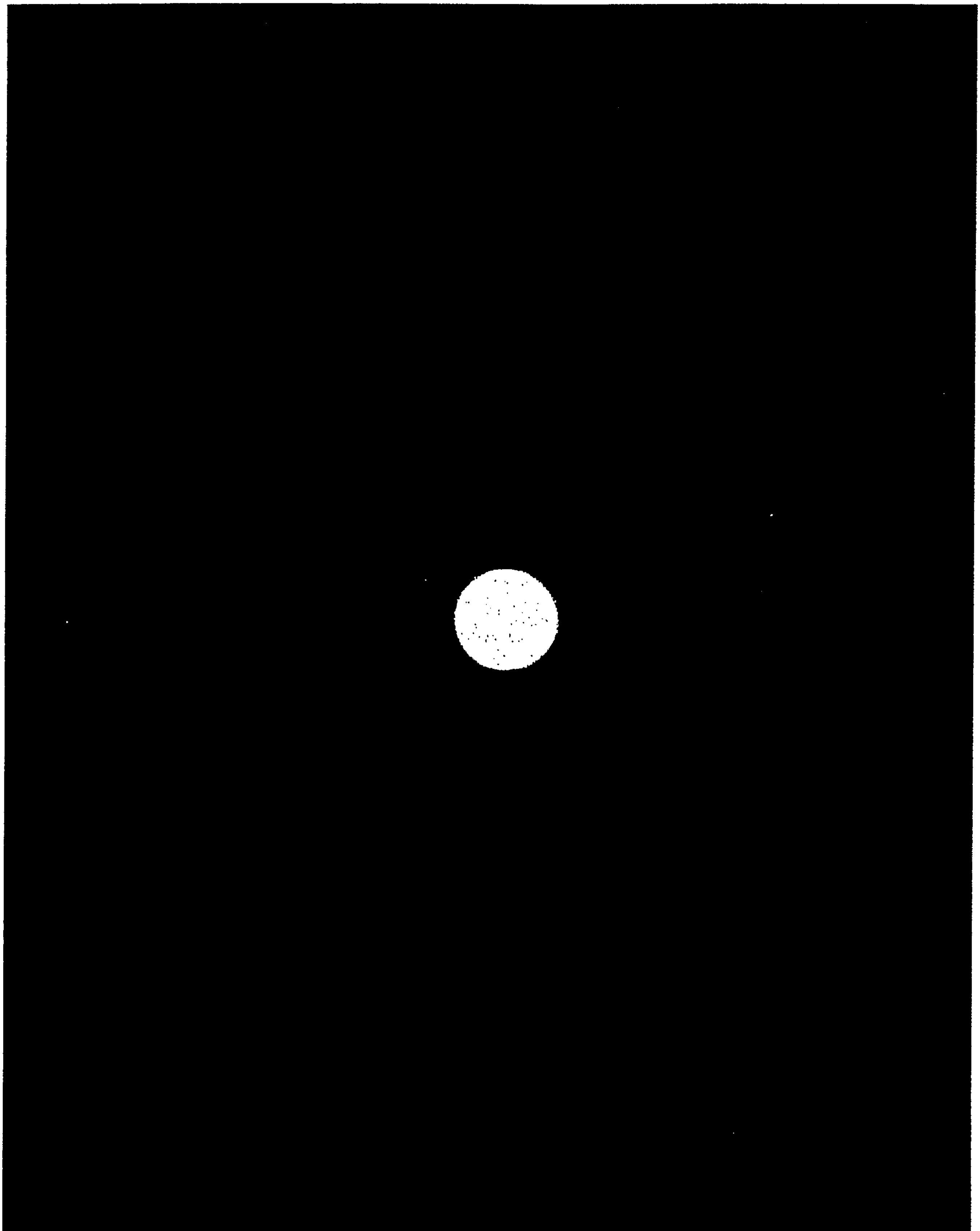

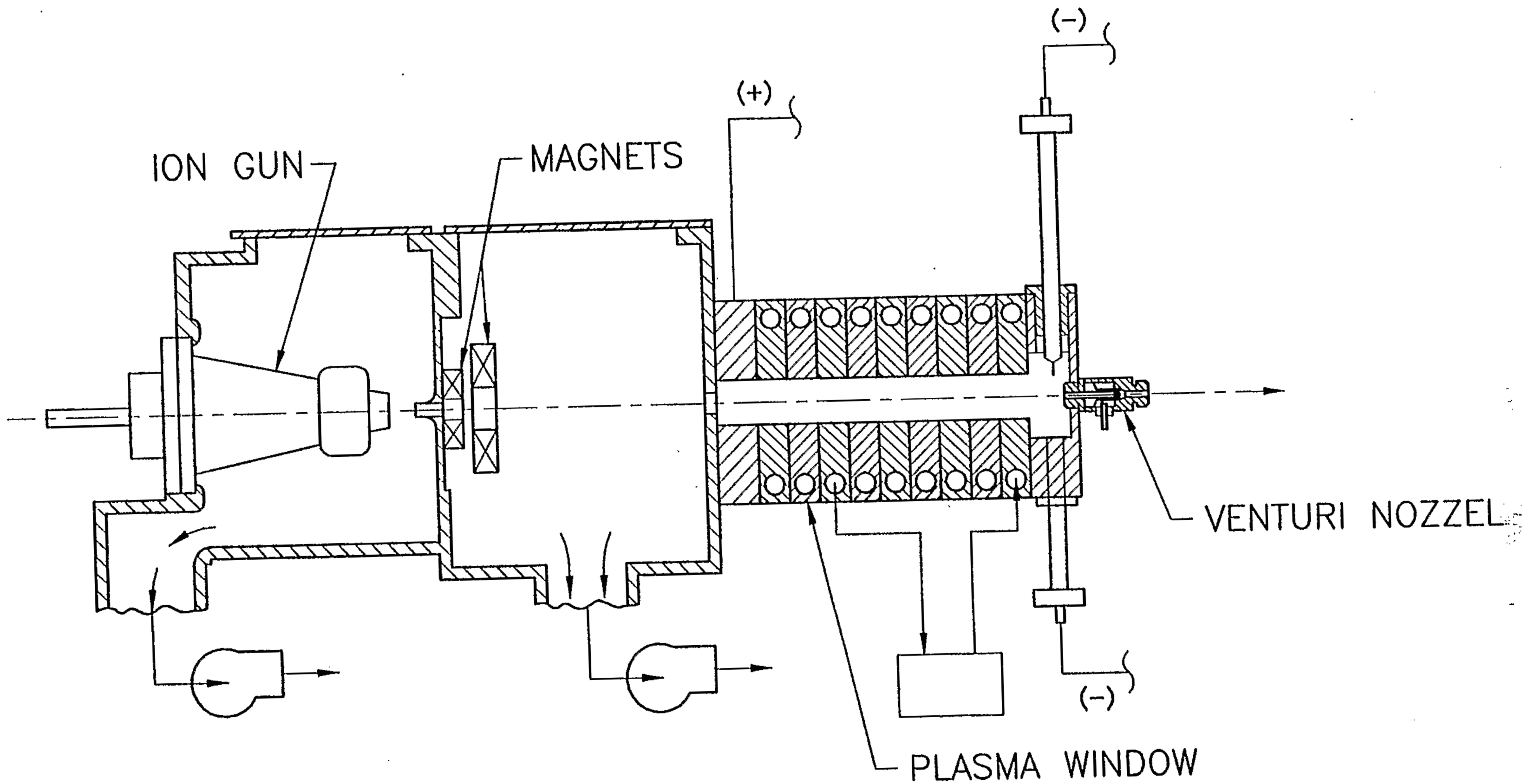


Figure 5